Journal of the European Ceramic Society 23 (2003) 675–683

www.elsevier.com/locate/jeurceramsoc

Viscous flow sintering of bioactive glass-ceramic composites toughened by zirconia particles

E. Verné[a,*], R. Defilippi[a], G Carl[b], C. Vitale Brovarone[a], P. Appendino[a]

[a]*Materials Science and Chemical Engineering Department, Polytechnic of Torino, C.so Duca degli Abruzzi 24, 10129, Turin, Italy*
[b]*Friedrich-Schiller-University Jena, Otto Schott Institute, Fraunhoferstraße 6, 07743 Jena, Germany*

Received 12 January 2002; accepted 12 May 2002

Abstract

In order to widen the application fields of a bioactive glass-ceramic (Bioverit®I), the possibility of preparing a glass-ceramic matrix biocomposite, toughened by zirconia particles, was investigated. Two kinds of biocomposites were prepared, using as reinforcing phase tetragonal yttria-stabilised zirconia (ZrO_2–3%Y_2O_3) and pure monoclinic zirconia particles, respectively. The composites were prepared by viscous flow sintering. The sintered composites were characterised by optical and Scanning Electron Microscopy (SEM), Energy Dispersion Spectroscopy (EDS) and X-Ray Diffraction (XRD). A mechanical characterisation of the sintered samples was carried out by means of Vickers indentations, Young's modulus measurements, fracture toughness and compressive strength determinations. The chemical stability of the samples was evaluated by soaking them in Ringer solution.

Keywords: Bioactive materials; Composites; Glass ceramics; Sintering; ZrO_2

1. Introduction

Nowadays, ceramic and glass-ceramic materials are currently used to repair bone and joint defects. Among them, zirconia is one of the most promising ceramic materials because of its exceptional inertness in biological fluids, its high fracture toughness and high flexural strength.[1] This ceramic, when put into the human body, undergoes to a morphological fixation with the tissues, i.e. a mechanical interlocking, and for that reason it is considered a "nearly inert bioceramic".

Several glass-ceramics show the property of directly bonding to the human tissues by interfacial reactions,[2,3] providing a bioactive fixation to the tissues. Generally, their mechanical properties, do not allow to use them for load-bearing applications. For this reason some authors addressed their efforts to toughen these materials by adding a second high-strength biocompatible phase.[4–11]

Bioverit®I is a machineable mica- and apatite-containing glass-ceramic, used for bone substitutions in several fields of human surgery. It is produced by a nucleation and growth heat treatment from the phase-separated silico-phosphate base-glass. To date,[12–14] the applications of pure Bioverit®I have been focused on small bone substitutions in orthopaedics, stomatology and for middle ear implants. In this work, the glass-ceramic Bioverit®I has been chosen as matrix for the preparation of bioactive composites, containing 20 wt.% zirconia particles as toughening phase. In this way the bioactive properties of the glass-ceramic could be combined with the high and reliable mechanical properties of zirconia. The composites were prepared by viscous flow sintering.

It is well known from literature[15,16] that pure zirconia presents a stable monoclinic structure at room temperature, which undergoes to a reversible structural transformation to a tetragonal phase when heated above 1000 °C. In details, this phase transformation is characterised by an evident hysteresis loop, since it happens at about 1100 °C during heating (monoclinic→tetragonal), and at about 950 °C during cooling (tetragonal→monoclinic). It is also known that this phase transformation produces an appreciable volume variation of about 7–9% (with expansion during cooling). The volume increase during cooling might induce

* Corresponding author. Tel.: +39-011-564-4687; fax: +39-011-564-4699.
E-mail address: enrica.verne@optics.polito.it (E. Verné).

0955-2219/02/$ - see front matter © 2002 Published by Elsevier Science Ltd.
PII: S0955-2219(02)00164-4

severe residual stresses if a zirconia-containing ceramic is heated at temperatures above the transformation range and than cooled down to room temperature. For this reason zirconia is frequently stabilised adding small amount of specific oxides aiming to partially maintain at room temperature the tetragonal phase in a metastable form.[17]

It is well documented the possibility of inducing the phase transformation by a mechanical stress.[18] This feature was successfully used to take advantage of it and to obtain a reinforcing mechanism in ceramic materials containing partially stabilised zirconia in the metastable tetragonal state.[19]

For comparative purposes, in this work, two different kind of zirconia particles were used as reinforcing phase in the sintered composites: yttria-stabilised tetragonal zirconia (ZrO_2–3%Y_2O_3) and pure monoclinic zirconia particles. The influence of the two different reinforcing phases on the sintering behaviour and the final properties of the two composites was investigated. The properties of the sintered composites were compared with those of pure Bioverit®I, sintered at identical time and temperature conditions.

2. Experimental

The starting glass for Bioverit®I glass-ceramic, with the wt.% composition of SiO_2 30.5, P_2O_5 11.4, Al_2O_3 15.5, CaO 14.4, MgO 14.8, K_2O 5.8, Na_2O 2.3, F-4.9, was melted at 1500 °C in a two stage melting process. The resulting glass was thermal treated for 1 h at 1000 °C to obtain the mica-apatite glass-ceramic.

The bulk glass-ceramic (named B1 from now on) was ball-milled and sieved to a bimodal particle size (70 wt.% 37÷105 μm, 30 wt.% < 37 μm) in order to optimise the particle distribution during the green compact preparation, according to the Furnas theory[20] on powder compacting, taking into account, for the green composite compacts, the zirconia wt.% and its particle size (< 44 μm). A structural characterisation was carried out on pure B1 and on the zirconia powders by X-Ray diffraction (XRD, Philips PW 1710), in order to determine the crystalline phases present before the sintering process. In the case of the two zirconia powders the amount of tetragonal and monoclinic phase was determinated using the Garvie and Nicholson method.[21]

Two different mixtures of glass-ceramic powders and reinforcing phase were obtained by the addition to B1 of 20 wt.% of Yttria-stabilised zirconia (ZrO_2–3% Y_2O_3, named Y-PSZ in this work, spherical granulated particles) and pure zirconia particles (obtained by atomization, named MZ in this work) (Tosoh).

The mixtures were prepared in a 15 ml ethanol suspension, and stirred until complete evaporation of the solvent. Cylindrical green compacts (3.14 cm diameter, 0.3–1.4 cm high, 5–25 g weight) of B1, B1/Y-PSZ and B1/MZ were prepared by uniaxial cold pressing of the mixed powders. Pressures ranging from 50 to 175 MPa were investigated, and the pressure of 100 MPa was finally chosen as the best compromise between high apparent density (61% in respect of the theoretical one) and absence of defects and cracks in the green compacts.

The linear shrinkage of each kind of green compact was determined by Hot Stage Microscopy (Leitz II A) on 3×3×3 mm^3 greens in the temperature range between 25 and 1150 °C. The sintering time and temperature parameters were optimised by performing several isothermal sintering processes in the temperature range where the highest shrinkage was observed (from 1040 to 1130 °C), for different times (0.5–4 h).

Density measurements (Archimede's method) were performed on each sintered sample in order to evaluate the degree of densification. The measured density of each sintered specimen (ρ_m) was compared with the theoretical one (ρ_{th}). The latter, in the case of the sintered composites, was calculated by using the mixtures law:

$$\rho_c = \rho_{BI}\chi_{BI} + \rho ZrO_2 \chi ZrO_2$$

$$\rho ZrO_2 = \rho_t ZrO_2 \chi_t ZrO_2 + \rho_m ZrO_2 \chi_m ZrO_2$$

where:

ρ_c	density of composite;
ρ_{BI}	density of Bioverit®I;
χ_{BI}	volume fraction of Bioverit®I;
$\rho_t ZrO_2$	density of tetragonal zirconia;
$\chi_t ZrO_2$	volume fraction of tetragonal zirconia;
$\rho_m ZrO_2$	density of monoclinic zirconia;
$\chi_m ZrO_2$	volume fraction of monoclinic zirconia.

The values of $\chi_m ZrO_2$ and $\chi_t ZrO_2$ were determined by means of the Garvie–Nicholson method. The morphology of each sintered sample was observed by means of optical microscopy and Scanning Electron Microscopy (SEM, Philips 525 M). Compositional (EDS, EDAX 9100) and phase (XRD, Philips 1810) analyses were performed in order to test if any modification occurred in the glass-ceramic matrix and in the zirconia particles during the sintering process.

Each kind of sintered composite was mechanically tested by observing the propagation path of some cracks induced by Vickers indentations. The Young's modulus was determined by means of resonance (Grindosonic Lemmens-Electronika), following the ASTM C 623–71 Standard Test Method.

The fracture toughness (K_{IC}) was determined by an indentation technique, using the following formula:[22,23] $K_{IC} = A(E/H)^{1/2}(P/c_0^{3/2})$, where A is a constant (=0.016) not depending on the tested material, E is the Young's Modulus of the material, H the Vickers hardness of the material, P the indentation load, c_0 the average value of

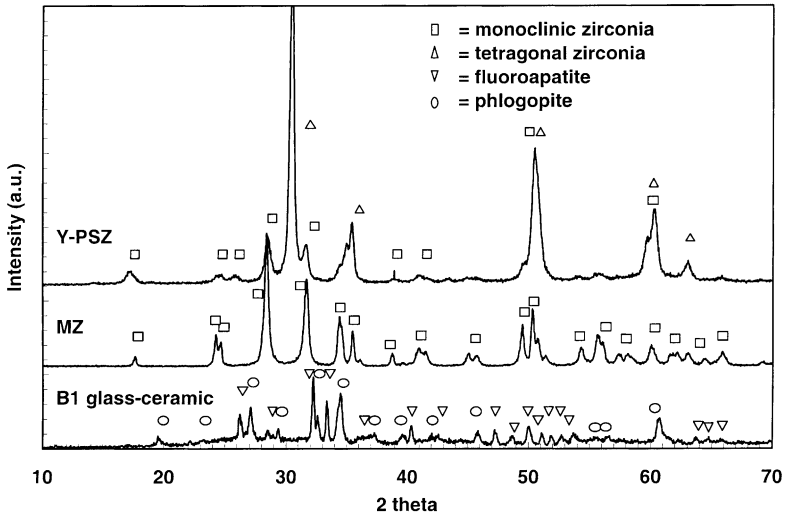

Fig. 1. XRD patterns of B1 glass-ceramic, Y-PSZ powders and MZ powders.

the cracks length, measured from the centre of each indent. The compressive strength of the sintered samples was evaluated by using a Schenck–Trabel equipment on cubic specimens ($10\times10\times10$ mm^3 size) obtained by cutting the 1.4 cm high sintered cylinders, following the indications of the ASTM C773–88 Standard Test Method (the method was modified for the specimens geometry because it was not possible to prepare cylindrical specimens, so the results reported in this work have only comparative purposes).

The surface reactivity of the sintered samples was evaluated by soaking them in Ringer's Solution (NaCl 9.00 g; $NaHCO_3$ 0.20 g; KCl 0.43 g; $CaCl_2$ 0.24 g; distilled water to 1 dm^3), up to 14 days: samples of each composite were soaked in 50 ml of solution, in polyethylene bottles at 37 °C. Morphological (SEM), compositional (EDS) and phase (XRD) analyses were performed on the samples after soaking in the solution.

Three point bending measurements were performed on $20\times2\times2$ mm^3 size composite bars, by using a material testing machine, Zwick 1445 (1 mm/min of deformation rate). This test was performed on both B1/Y-PSZ and B1/MZ sintered samples. Some measurements of flexural strength were performed on B1/Y-PSZ composite also after soaking in Ringer's solution, in order to evaluate the effect of this simulated biological medium on its mechanical behaviour. At least 14 specimens were tested for each mechanical characterisation, and an average value is reported in this work for each kind of material.

3. Results

The XRD characterisation of the glass-ceramics and zirconia powders gave the results reported in Fig. 1. The crystalline phases individuated in the B1 glass-ceramic are fluorapatite and phlogophite. In the Y-PSZ powders 20% monoclinic and 80% thetragonal zirconia were individuated, while in the MZ powders only monoclinic zirconia was found.

Fig. 2 shows the linear shrinkage of B1, B1/Y-PSZ and B1/MZ green compacts respectively, obtained by hot stage microscopy. For each kind of compact the densification occurred starting from 900 °C with an asymptotic behaviour up to temperatures close to the liquidus range. For this reason the sintering temperature range was chosen between 1040 and 1100 °C, in order to assure the maximum shrinkage of the samples. Different sintering times were investigated: 30, 60, 120, 240 minutes in air.

The average density values for each kind of sintered samples are summarised in Table 1. The density values

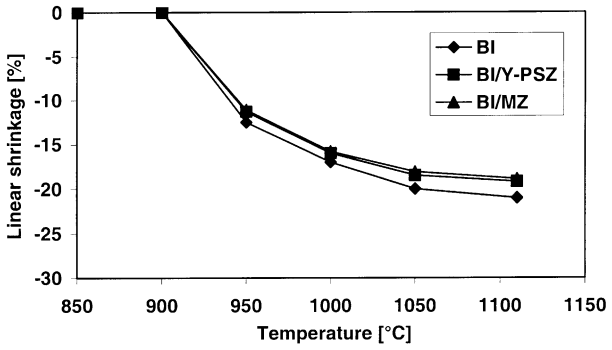

Fig. 2. Linear shrinkage of B1, B1/Y-PSZ and B1/MZ green compacts.

Table 1
Density average values of the samples sintered at 1100 °C for 2 h

	ρ_{th} (g/cm^3)	ρ_m (g/cm^3)	ρ_m/ρ_{th} (%)
Bioverit®I	2.72	2.66	97.8
Bioverit®I/Y-PSZ	3.03	2.95	97.4
Bioverit®I/MZ	3.09	2.99	96.8

were reported as a function of the sintering time and temperature conditions (see graphic of the B1/Y-PSZ reported in Fig. 3).

By comparing these values, an optimised sintering schedule of 1100 °C for 2 h was selected. The heating rate from room temperature to 1100 °C and the cooling rate after sintering was of 10 °C/min (B1, B1/Y-PSZ) and of 5 °C/min (B1/MZ). These heating and cooling rates were chosen in order to avoid as much as possible any residual stress due to fast temperature modifications, especially in the case of B1/MZ, because of the reversible phase transformation (monoclinic→tetragonal) which could occur in the chosen temperature range with volume variation. On the samples sintered at the optimised conditions, an XRD characterisation was carried out, in order to observe if any additional phase was formed in the samples due to the sintering process. Fig. 4 reports the XRD patterns of sintered B1, B1/Y-PSZ and

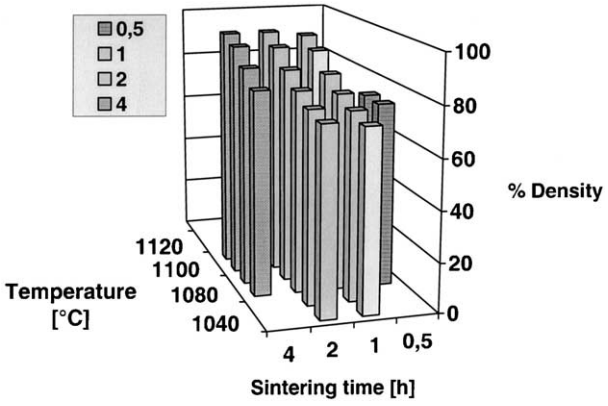

Fig. 3. Density of the sintered B1/Y-PSZ sample as a function of time and temperature.

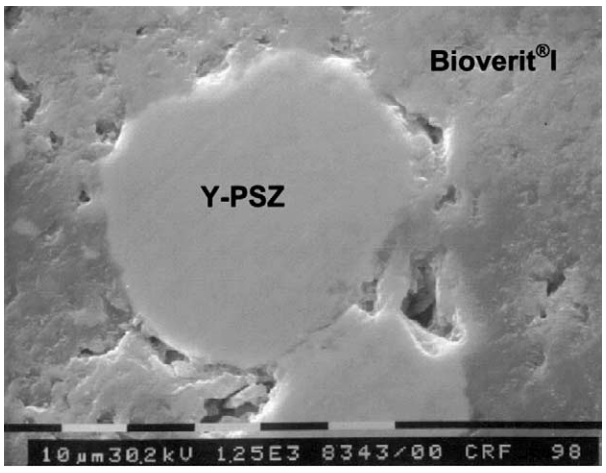

(a)

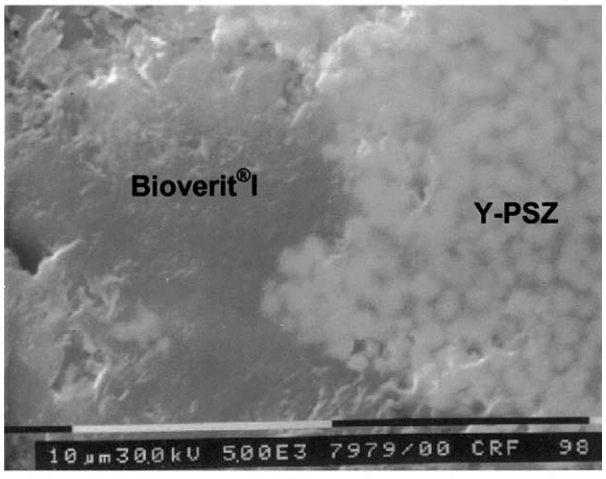

(b)

Fig. 5. Polished cross section of the B1/Y-PSZ composite (a); detail of the interface between the B1 matrix and a Y-PSZ particle (b).

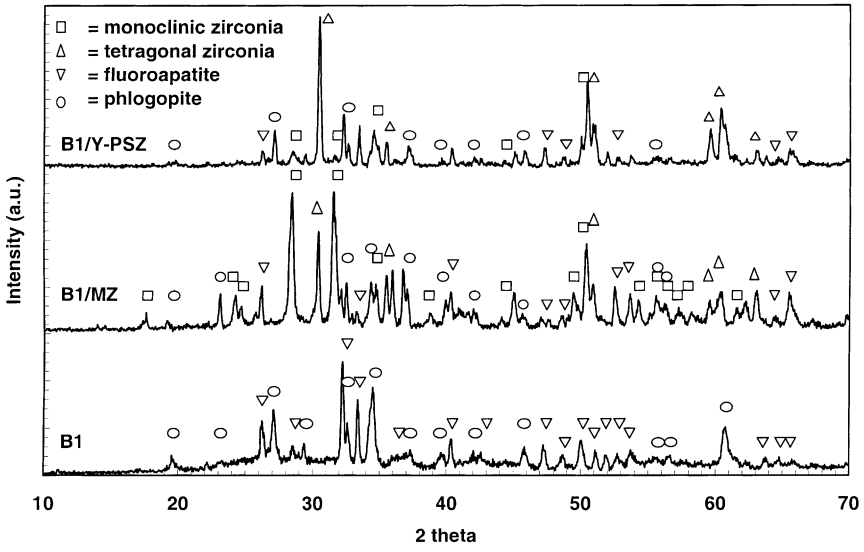

Fig. 4. XRD patterns of B1, B1/Y-PSZ and B1/MZ, sintered at 1100 °C for 2 h.

B1/MZ respectively. No additional phases were individuated in the sintered B1 sample. The B1/Y-PSZ composite only showed the signals of fluorapatite, phlogophite, monoclinic zirconia and tetragonal zirconia. Using the Garvie and Nicholson method, the amount of monoclinic and tetragonal zirconia was determined: it was the same as in the unfired zirconia powders (20% ZrO_2^m–80% ZrO_2^t). The B1/MZ composite showed the signals of fluorapatite, phlogophite monoclinic zirconia and tetragonal zirconia (25.5% ZrO_2^t–74.5% ZrO_2^m).

The morphological characterisation of the sintered samples revealed some differences between the two kinds of composites. The B1/Y-PSZ composite shows a good interface between the glass-ceramic matrix and the zirconia particles, with very few pores. The zirconia particles show an almost spherical geometry and are well embedded in the glass-ceramic matrix. The residual porosity is sometimes localised at the interface between the matrix and the dispersed phase.

Fig. 5a shows a polished cross section of this composite. In Fig. 5b a detail of the interface between the B1 matrix and a Y-PSZ particle is reported: the microstructure of the zirconia particle is evidenced due to a certain infiltration of the residual glassy phase of the glass-ceramic B1. This feature is observable only at high magnifications.

A general view of a B1/MZ composite is shown in Fig. 6. This composite shows a higer infiltration of the matrix inside the zirconia particles, which lead to a partial dispersion of the MZ particles into the B1 matrix: they partially loose their globular geometry and appear as "agglomerates" of sub-micronic zirconia granules.

Fig. 7a shows a polished section of a B1/Y-PSZ composite, after chemical etching by a 1:1 HF/HNO_3 aqueous solution (5 vol.%). The picture evidences the crystalline phases of the glass-ceramic matrix and the zirconia particles. A polished section of the B1/MZ composite, after chemical etching by a 1:1 HF/HNO_3 aqueous solution (5 vol.%) is shown in Fig. 7b. The zirconia particle is completely divided in small grains, due to the chemical etching of the amorphous phase infiltrated from the matrix.

EDS analyses were performed on the glass-ceramic matrix and on the zirconia particles, in each kind of composites, in order to evaluate the degree of infiltration of the matrix into the zirconia particles and to verify if any Zr^{4+} diffused into the glass-ceramic matrix. The results are summarised in Table 2. In the case of B1/Y-PSZ composite, a little amount of Zr^{4+} was detected in the glass-ceramic matrix (6.1 wt.%), and similarly in the zirconia particles a certain amount of Si and P was found. In the case of B1/MZ composite the comparison between EDS result on the matrix and on the particles was difficult to achieve, because of the higher dispersion of zirconia particles into the matrix, but it evidenced a deeper infiltration of a Si and P rich phase inside the zirconia particles and the presence of Zr

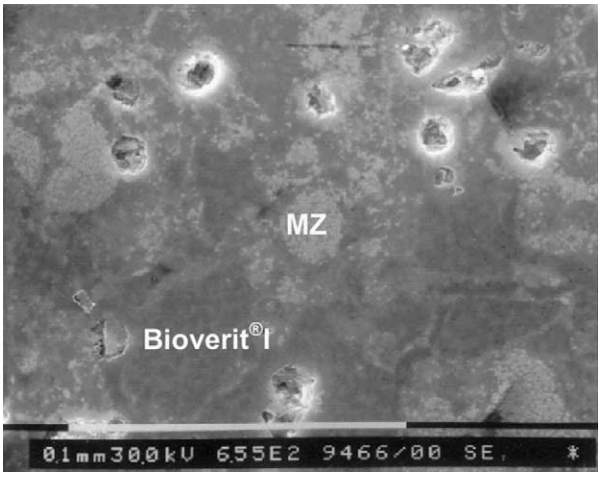

Fig. 6. General view of a B1/MZ composite polished section.

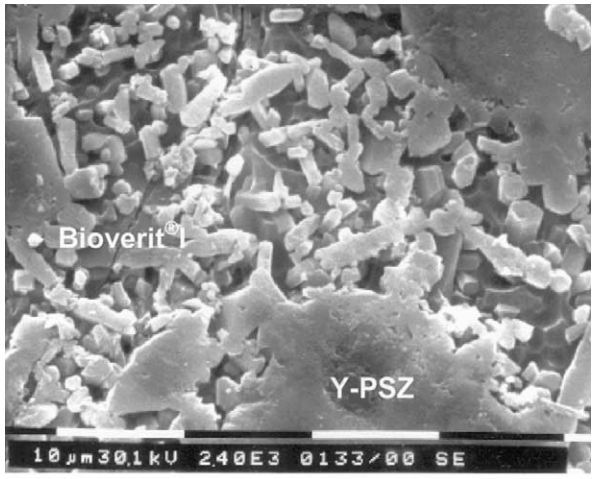

(a)

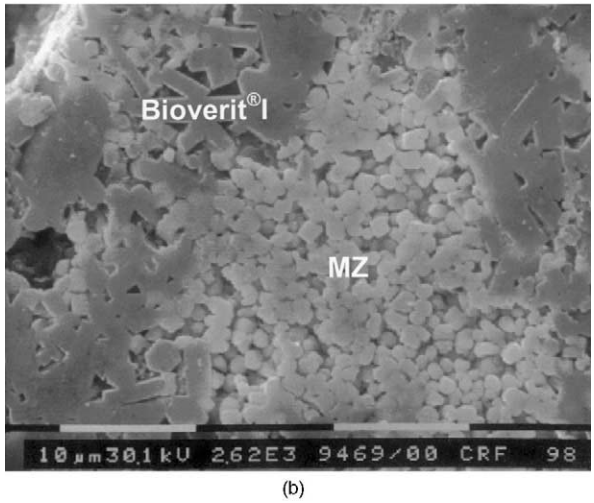

(b)

Fig. 7. Polished section of a B1/Y-PSZ composite, after chemical etching (a) and of the B1/MZ composite, after chemical etching (b).

Table 2
EDS analyses performed on the glass-ceramic matrix and on the zirconia particles of the B1/Y-PSZ composite

Element	Glass-ceramic matrix (wt.%)	Y-PSZ particles (wt.%)
Si	22.7	7.5
Ca	20.2	<2
Na	2.5	<1
K	6.8	<1
Mg	12.7	<2
Al	12.3	<2
F	3.6	<1
P	11.4	29.7
Zr	7.8	55.5
Y	–	2.1

in the glass-matrix. It was not possible, neither by average nor by punctual EDS analyses, to distinguish between the dispersed ZrO_2 grains and the Zr^{4+} eventually diffused into the B1 matrix.

The mechanical behaviour of the sintered composites was preliminary investigated by observing the induced crack pattern, after Vickers indentations performed with loads from 98.07 to 196.14 N. The composites showed a tougher behaviour in comparison with the pure glass-ceramic, as evidenced by comparing Fig. 8a–c. In the pure glass-ceramic (Fig. 8a) a brittle fracture can be observed, with straight and ~500 micron long crack propagation from the indent corners. The B1/Y-PSZ composite did not show straight cracks (Fig. 8b), but only short cracks stopped or deviated by zirconia particles. Moreover, in the composite the indent size is larger than in the pure glass-ceramic. A similar behaviour was observed in the B1/MZ composite (Fig. 8c).

Fig. 9a shows a detail of a polished cross section of a B1/Y-PSZ composite after Vickers indentation with 196.14 N kg load. The induced crack propagates around the zirconia particles, being deviated by them. In Fig. 9b a polished cross section of a B1/MZ composite indented with the same load is reported. In this case the crack propagate across the zirconia particle, being deviated by the micronic grains (which are evidenced by the matrix infiltration).

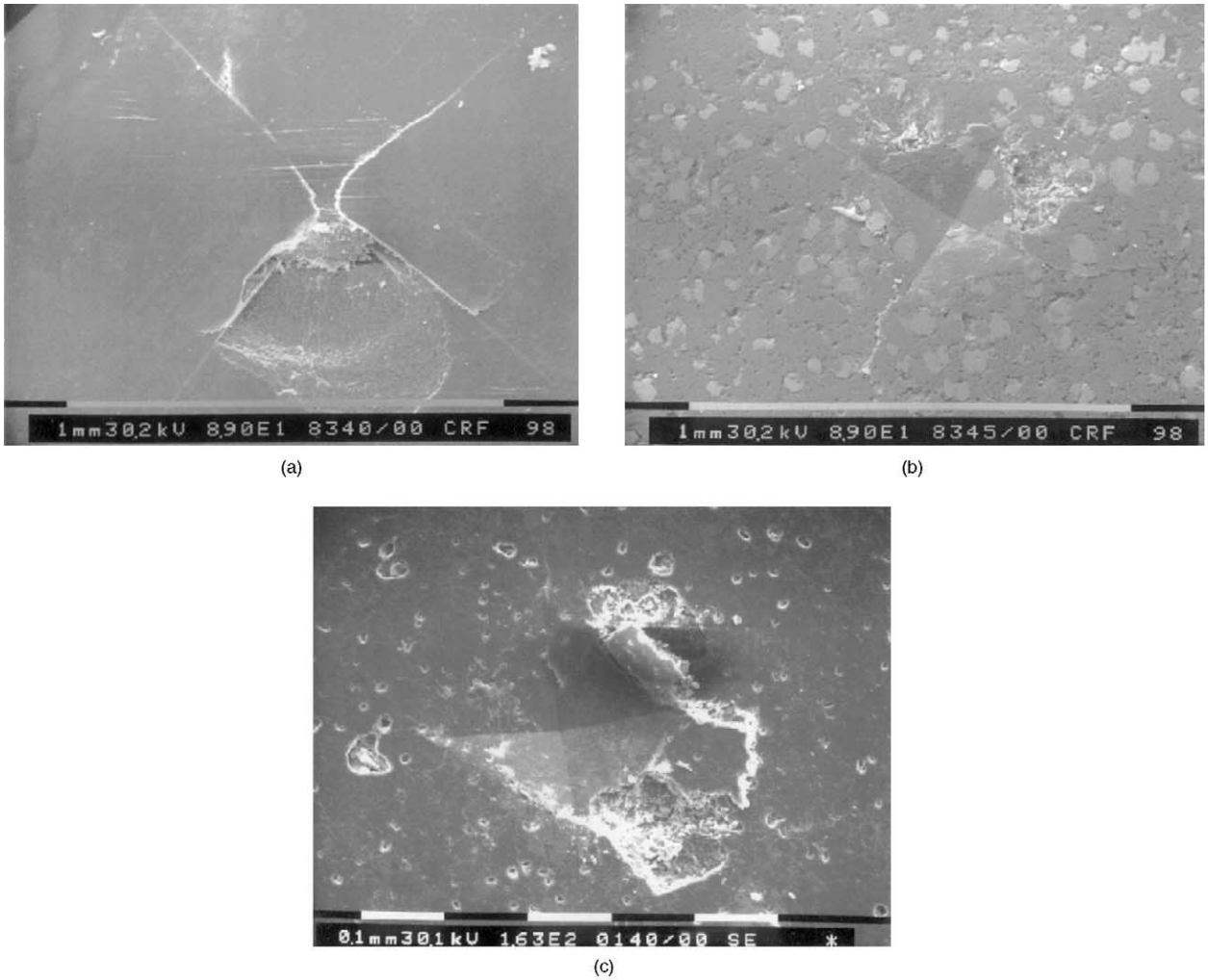

Fig. 8. Induced crack propagation on pure glass-ceramic (a), the B1/Y-PSZ composite (b), the B1/MZ composite (c).

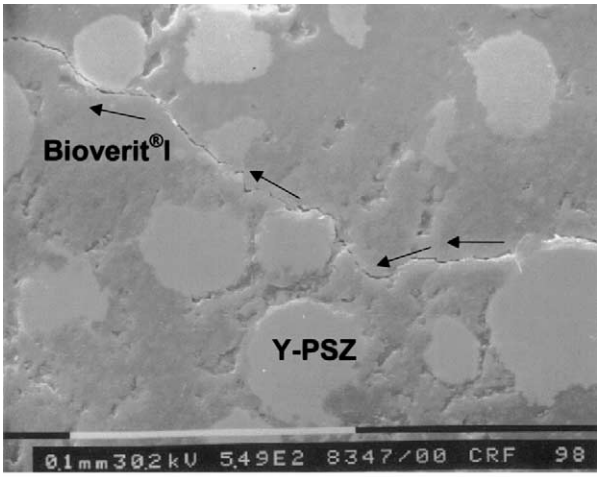

(a)

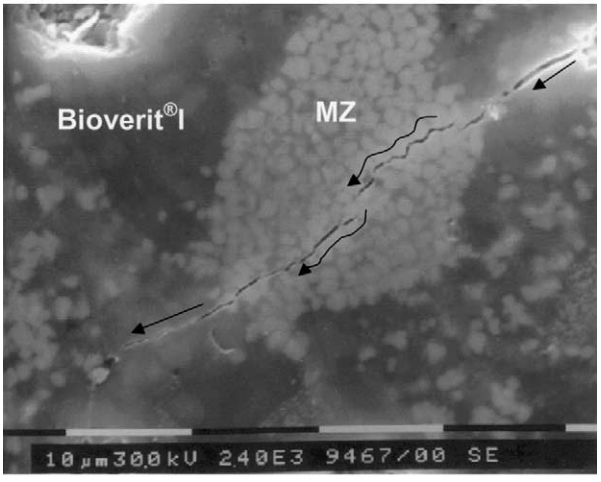

(b)

Fig. 9. Detail of polished cross sections of a B1/Y-PSZ composite (a) and a B1/MZ composite (b) after Vickers indentation (196 N load).

The results of the mechanical characterisation performed on the sintered samples are reported in Table 3. No significative variations of Young's modulus were observed for the B1/MZ composite in comparison with the pure sintered B1, while in the case of the B1/Y-PSZ composite a lower value was determined. An increase of compressive strength was evident in the case of B1/MZ, compared to the pure sintered B1. The fracture toughness of both the composites was higher than that of the pure sintered B1, with a very high value for the B1/Y-PSZ. A higher value of flexural strength was determined in the B1/MZ composite in respect to the B1/Y-PSZ one.

After 2 weeks of soaking in Ringer solution, the sintered composite samples were characterised by a morphological and structural point of view. No signs of degradation were detected. The surface of each kind of composite did not reveal appreciable modification (see Fig. 10a and b). The XRD pattern of both B1/Y-PSZ and B1/MZ composites did not revealed additional phases or differences in the peak intensities of the original

Table 3
Mechanical test results on pure sintered B1, B1/Y-PSZ and B1/MZ

	E (GPa)	σ_{comp} (MPa)	σ_{flex} (MPa)	K_{IC} (MPa×m$^{1/2}$)
Sintered Bioverit®I	77	182	–	1.3
Bioverit®I/Y-PSZ	59	118	48.7	2.5
Bioverit®I/MZ	78	232	96.3	1.7

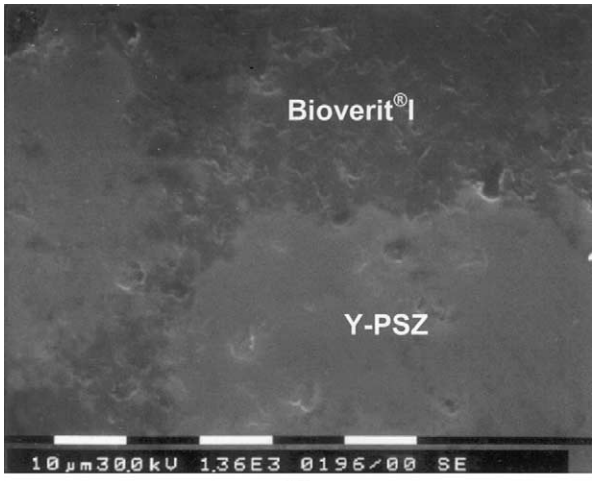

(a)

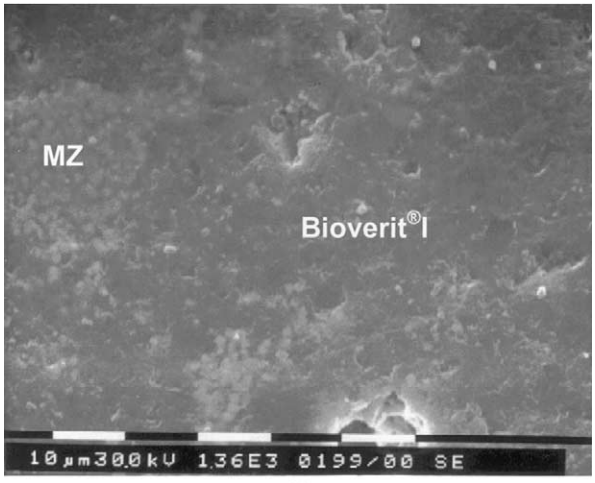

(b)

Fig. 10. Surface of a B1/Y-PSZ composite (a) and of a B1/MZ composite (b) after 2 weeks of soaking in Ringer's solution.

phases. The flexural strength measurements performed on B1/Y-PSZ composite gave almost the same average results before and after soaking in the solution (before: 48.7 MPa, after: 47.8 MPa).

4. Discussion

The sintering behaviour and the final properties of the composites prepared in this work by viscous-flow sintering were deeply influenced by the different nature of the

dispersed phase: Yttria-stabilised zirconia in a case (B1/Y-PSZ) and pure monoclinic zirconia in the other (B1/MZ).

The use of whether partially stabilised tetragonal zirconia particles or not stabilised monoclinic ones in the two kind of composites realised in this work, involved some differences in the sintered samples. These differences are likely to be related to the different behaviour during heating of the two dispersed phases, and to their different tendency to be infiltrated by the amorphous phase.

During the sintering process of the composite B1/Y-PSZ no phase transformations were observed (compare Figs. 1 and 4). On the contrary, in the case of B1/MZ a phase transformation occurred and it strongly affected the final properties of the composite, i.e. its morphology and its mechanical behaviour.

By a morphological point of view, the sintered samples show some differences one from each other. The infiltration phenomenon was particularly evident in the B1/MZ composite, where the zirconia particle's morphology resulted not well defined. Each zirconia particle can be considered a composite itself, because of the infiltration of P_2O_5/SiO_2 rich amorphous phase, which leads to a partial spreading of each particle into agglomerates of small zirconia grains (about 1 μm size).

Most of the differences among the sintered samples concerned the mechanical behaviour.

The Young's modulus of the composite B1/MZ is higher than that of B1/Y-PSZ and close to the not-reinforced glass-ceramic one. This feature is likely to be related to the more uniform distribution of the micronic zirconia granules (i.e. better stress transmission between the B1 matrix and the dispersed phase) of B1/MZ compared to B1/Y-PSZ (in the latter case the zirconia particles, not disgregated, present the original coarser morphology). Moreover, in the B1/Y-PSZ composite the residual porosity is sometimes localised at the interface between the matrix and the dispersed phase, leading to a less effective stress transfer.

Further differences are evidenced by the analysis of the induced crack patterns and of the K_{IC} values. Both the composite materials present K_{IC} values higher than that of the pure glass-ceramic. This is particularly evident in the case of B1/Y-PSZ, according to its low Young's modulus. Moreover, the Vickers indentations revealed a different mechanical behaviour of the pure B1 in comparison to the two composites. Some indentations at 196 N load on the sintered pure glass-ceramic produced the propagation of very long crack and brittle fracture of the surface around the indent. On the contrary the sintered composites showed a tougher behaviour: very few cracks and no brittle behaviour were observed on indenting the sample with the same load used for the not reinforced B1.

The toughening mechanism was very different for the two composites. In the B1/Y-PSZ composite the crack deflection mechanism around the zirconia particles is clearly evident (see Fig. 9a). In the B1-MZ a different mechanism can be noticed: the cracks are stopped by crossing through the zirconia agglomerates, and during their path they are deflected by the small zirconia granules (Fig. 9b). In this latter case the fracture energy absorption is likely to be related both to crack deflection around the micronic zirconia granules and to phase transformation from the metastable tetragonal to a monoclinic structure which could occur when a crack tip interact with small tetragonal zirconia grains. Since the firing treatment was carried out above the transformation temperature, the monoclinic zirconia of the B1-MZ composite was transformed to the tetragonal form. This transformation should be reversible, but during cooling it was prevented by the viscosity increase of the densified glass-matrix, as can be evidenced by the higher volume fraction of tetragonal zirconia in the sintered B1-MZ composite compared to the green one. The transformation toughening mechanism could be observable only in the B1-MZ sintered composite (and not in the B1/Y-PSZ one) because only in this case the zirconia particles are highly infiltrated by the glass-matrix, leading to the above mentioned agglomerates, which are easily crossed by the crack tips.

The compression strength results for the B1 glass-ceramic and the two composite revealed remarkable differences, according to these considerations. The B1-MZ composite showed a higher value than the not reinforced glass-ceramic and the B1/Y-PSZ composite. This latter one is even less resistant than the pure B1. The same trend is observable in the flexural strength values of the two composites. The better particle dispersion and their smaller size in the B1-MZ composite compared to the B1/Y-PSZ one can explain these differences. It seems that the pure crack deflection mechanism noticed in the B1/Y-PSZ is not so effective to induce a good toughening effect. For this reason this composite is not useful for applications that involve strong compressive stresses. The residual porosity localised at the interface between the matrix and the zirconia particle (Fig. 5a) can strongly affect the mechanical properties in terms of Young's modulus, flexural strength and compressive strength, and can also explain the high value of K_{IC} as it influences the induced crack propagation. On the contrary, no residual porosity is observable inside the zirconia agglomerates of the B1-MZ composite, leading to a more effective fracture energy dispersion.

The morphological and mechanical characterisation after soaking in Ringer solution was useful to state that the sintered composites can be considered as durable material in physiological media.

5. Conclusions

A pressureless viscous flow sintering process was used to prepare two kinds of Bioverit®I-matrix composites

reinforced by yttria-stabilised zirconia (B1/Y-PSZ) and pure zirconia particles (B1-MZ) respectively. The mechanical characterisation showed a better behaviour of the composite containing pure zirconia particles as starting dispersed phase. The best performance of this composite is related to the high dispersion of the zirconia particles in the matrix (due to the infiltration in the starting particles of an amorphous phase) and to the best effectiveness of these small grains in the toughening mechanism. A partial contribute of a phase transformation mechanism could be supposed, on the basis of the morphological and structural characterisation of the B1-MZ composite. By soaking the composites in Ringer solution it was evidenced their chemical stability in physiological media.

References

1. Hulbert, S. F., The use of alumina and zirconia in surgical implants. In *An Introduction to Bioceramics*, ed. L. L. Hench and J. Wilson. Advances Series in Ceramics, Vol. 1. World Scientific Publishing, 1993, p. 25.
2. Hench, L. L., Bioceramics. *J. Am. Ceram. Soc.*, 1998, **81**(7), 1705–1728.
3. Cao, W. and Hench, L. L., Bioactive materials. *Ceram. Int.*, 1996, **22**, 493–507.
4. Ferraris, M., Rabajoli, P., Brossa, F. and Paracchini, L., Vacuum plasma spray deposition of titanium particle/glass-ceramic matrix biocomposites. *J. Am. Ceram. Soc.*, 1996, **79**(6), 1515–1520.
5. Verné, E., Ferraris, M., Ventrella, A., Paracchini, L., Krajewski, A. and Ravaglioli, A., Sintering and plasma-spray deposition of bioactive glass-matrix composites for biomedical applications. *J. Eur. Ceram. Soc.*, 1998, **18**(4), 363–372.
6. Verné, E., Ferraris, M. and Jana, C., Pressureless sintering of Bioverit®III/Ti particle biocomposites. *J. Eur. Ceram. Soc.*, 1999, **19**, 2039–2047.
7. Verné, E., Ferraris, M., Jana, C. and Paracchini, L., Bioverit®I base glass/Ti particulate biocomposite: ''in situ'' vacuum plasma spray deposition. *J. Eur. Ceram. Soc.*, 2000, **20**, 473–479.
8. Kasuga, T., Nakajima, K., Uno, T. and Yoshida, M., Preparation of zirconia-toughened bioactive glass-ceramic composite by sinter-hot isostatic pressing. *J. Am. Ceram. Soc.*, 1992, **75**(5).
9. Kasuga, T., Yoshida, M., Uno, T. and Nakajima, K., Preparation of zirconia-toughened bioactive glass-ceramics. *J. Mater. Sci.*, 1988, **23**, 2255–2258.
10. Ducheyne, P., Marcolongo, M., Shepers, E., Bioceramic composites. In *An Introduction to Bioceramics*, ed. L. L. Hench and J. Wilson. Advances Series in Ceramics, Vol. 1. World Scientific Publishing, 1993, p. 281.
11. Van Hove, L., Schepers, E., Ducheyne, P., Titanium fiber reinforced bioactive glass-composite implants. In *Bioceramics*, Vol. 6, ed. P. Ducheyne and D. Christiansen, Butterworth-Heinemann, 1993, pp. 319–325.
12. Höland, W. and Vogel, W., Machineable and phosphate glass-ceramics. In *An Introduction to Bioceram.*, ed. L. L. Hench and J. Wilson. World Scientific, Singapore, 1993, pp. 125–137.
13. Schubert, T., Purath, W., Liebscher, P. and Schulze, K. J., Klinische Indikationen für die Anwendung der Janaer Bioaktiven Maschinell Bearbeitbaren Glaskeramik in der Orthopädie und Traumatologie. *Beiträge Orth. Traumatol.*, 1988, **35**, 7–16.
14. Pinkert, R., Naumann, K. and Vogel, W., Individuelle Herstellung Enossaler Zahnimplantate aus der Maschinellen Bearbeitbaren Glaskeramik Jena. *Philip Journal*, 1987, **6**, 339–342.
15. Lynch, C., Vahldiek, F. and Robinson, L., Monoclinic-Tetragonal transition of zirconia. *J. Am Ceramic Soc.*, 1961, **44**(3), 147–148.
16. Yoshimura, M., Phase stability of zirconia. *Ceram. Bull.*, 1988, **67**(12).
17. Heathcote, R., Zirconium oxide. *Ceram. Bull.*, 1992, **71**(5), 822–824.
18. Porter, D., Evans, A. and Heuer, A., Transformation-toughning in partially stabilized zirconia (PSZ). *Acta Metall.*, 1979, **27**, 1649–1654.
19. Becher, P. F., Toughening behaviour in ceramics associated with the transformation of tetragonal ZrO_2. *Acta Metall.*, 1986, **34**(10), 1885–1891.
20. Reed, J. S., In *Introduction to the Principles of Ceramic Processing*. J. Wiley & Sons, New York, 1988, pp. 188–190.
21. Garvie, R. and Nicholson, P., Phase analysis in zirconia system. *J. Am. Ceram. Soc.*, 1972, **55**(6), 303–305.
22. Rizkalla, A. S., Jones, D. W. and Miller, R. P., Evaluation of indentation fracture toughness methods for glass biomaterials. *Br. Ceram. Trans.*, 1996, **95**(4), 151–156.
23. Swain, M. V. and Claussen, N., Comparison of K_{IC} values for Al_2O_3–ZrO_2 composites obtained from notched-beam and indentation strength techniques. *Am. Ceram. Soc. Comm.*, 1983, **Feb.**, C–27.